Infrared spectroscopic analysis of zircon: Radiation damage and the metamict state

2001 J. Phys.: Condens. Matter 13 3057

(http://iopscience.iop.org/0953-8984/13/13/317)

INSTITUTE OF PHYSICS PUBLISHING JOURNAL OF PHYSICS: CONDENSED MATTER

J. Phys.: Condens. Matter **13** (2001) 3057–3071 www.iop.org/Journals/cm PII: S0953-8984(01)20082-4

Infrared spectroscopic analysis of zircon: Radiation damage and the metamict state

Ming Zhang[1] **and Ekhard K H Salje**

Mineral Physics, Department of Earth Sciences, University of Cambridge, Downing Street, Cambridge CB2 3EQ, UK

E-mail: mz10001@esc.cus.cam.ac.uk

Received 14 December 2000, in final form 23 February 2001

Abstract

Radiation damage and the nature of the metamict state in natural zircons were studied and analysed using reflection and absorption infrared spectroscopy. IR bands of crystalline zircon in the far infrared region remain detectable in highly metamict samples. This suggests that some local order or short-range order persists around Zr atoms in the amorphized phase. Signals due to Si–O–Si linkages, which do not exist in crystalline zircon, were observed in the regions of 500–800 cm^{-1} and 1000–1300 cm^{-1}. The results suggest the appearance of high-Q species and a complex polymerization state in the metamict state. The dielectric constant ($\varepsilon = \varepsilon' + i\varepsilon''$) and energy loss function ($-\mathrm{Im}(1/\varepsilon)$) were obtained through Kramers–Kronig analysis.

Radiation damage leads to significant and continuous variations in ε and $-\mathrm{Im}(1/\varepsilon)$. IR spectra of damaged samples were analysed using the effective-medium approach. It was found that IR signals of damaged zircons consist of two principal components: one with broad spectral features from the amorphized/metamict material and the other with relatively sharp lines from crystalline material with various degrees of structural distortion. The former signals increase in intensity with increasing dose while the latter decrease in intensity. The signals from the amorphized phase have been detected in samples with radiation dose as low as 1.5×10^{18} α-events g^{-1}. The dose dependence of the fraction of the amorphized phase was extracted. The result confirms earlier analysis in x-ray diffraction and NMR studies. The IR data show a feature that may be due to the existence of an intermediate phase in moderately damaged samples. An extra, sharp IR band near 796 cm^{-1}, which shows no detectable orientation dependence, is observed in all the samples with intermediate degrees of damage and its intensity shows a systematic change with increasing dose—an increase followed by a decrease. This band is absent or very weak in both undamaged and very heavily damaged samples.

[1] Author to whom correspondence should be addressed.

0953-8984/01/133057+15$30.00

1. Introduction

Zircon ($ZrSiO_4$) is tetragonal with space group D_{4h}^{19} or $I4_1/amd$ and $Z = 4$ (Hazen and Finger 1979). The ideal structure consists of a chain of alternating, edge-sharing SiO_4 tetrahedra and ZrO_8 triangular dodecahedra extending parallel to the crystallographic c-axis. Zircon is widely used in the ceramic, foundry and refractory industries. It is also a phase extensively used in U/Pb radiometric age-dating. It is among several crystalline phases currently under consideration for the immobilization and disposition of high-actinide wastes. Natural zircon commonly contains U, Th and other rare earth elements. Due to radioactive decay of naturally occurring radionuclides and their daughter products in the ^{238}U, ^{235}U and ^{232}Th decay series, the structure of zircon can be heavily damaged over geological times, resulting in a partially aperiodic state, the so-called metamict state (Ewing 1994, Salje *et al* 1999).

We undertook this study with two main objectives. Firstly, we wished to gain a deeper understanding of what the local structure of amorphized/metamict phase is and what happens around Zr and Si atoms during metamictization as experimental controversies remain. It has been reported that in the metamict state the Zr–O distance decreases by 0.1 Å and that the coordination number of Zr decreases from 8 to 7 (Farges and Calas 1991). Earlier IR and Raman results did not seem to support a change of polymerization. Woodhead *et al* (1991) reported that the structure of metamict zircon consisted of distorted and disoriented isolated silica tetrahedra with few if any undisplaced Zr cations. Raman work of Nasdala *et al* (1995) revealed no indication of an amorphous phase. These authors did not find any evidence for an increasing polymerization of SiO_4 tetrahedra and they proposed that isolated SiO_4 groups, which could become distorted and tilted with increasing metamictization, were still isolated in the highly metamict state. On the other hand, more recent spectroscopic results have shown that Si–O interactions undergo dramatic changes indicating changes of their local environments. Raman data have revealed new broad Si–O stretching vibrations near 920 and 970 cm^{-1} related to the amorphized phase accompanied by sharp Raman signals from crystalline zircon (Zhang *et al* 2000c). Polarized IR reflectance data of Si–O vibration measured between 650 and 1400 cm^{-1} have shown new Si–O–Si linkages in metamict zircon (Zhang *et al* 2000b). Recent NMR data have showed that radiation damaged zircon samples gave new NMR signals (Farnan and Salje 2001). Secondly, we wished to investigate the impacts of radiation damage on dielectric properties of zircon, to estimate the fraction of amorphized phase as a function of radiation dose, and to compare the results with those obtained by x-ray diffraction (Ríos *et al* 2000) and NMR (Farnan and Salje 2001).

2. Samples and experiment

Natural zircons from different localities with a range of degree of radiation damage were used in this study. Most of them are gemstones. 32 among the total 38 samples were analysed previously by density measurement, instrumental neutron activation method, electron microprobe measurement, x-ray diffraction, HRTEM, Raman and infrared spectroscopy (Murakami *et al* 1991; Ellsworth *et al* 1994; Salje *et al* 1999; Ríos *et al* 2000; Zhang *et al* 2000a, b, c). The other samples were characterized using analytic methods: infrared spectroscopy, Raman spectroscopy, X-ray diffraction measurement, electron microprobe analysis and density measurement. Using the method of Murakamii *et al* (1991), radiation dose was obtained for Sri Lanka zircons with a defined geological age of 570 ± 20 million years (Holland and Gottfried 1955). The estimated uncertainty for the dose determination for these Sri Lanka zircons is less than 0.5×10^{18} α-events g^{-1}. For the samples from other localities, due to lack of information on their geologic ages the dose was obtained using the dose–cell

parameter relation of Holland and Gottfried (1955) and a dose–Raman peak parameter calibration for partly damaged zircons (Zhang *et al* 2000c). The dosage was also checked using the reflectivity and dose dependence obtained in this study from Sri Lanka zircons. The cell parameters and density as a function of the dose determined by the above methods are consistent with those reported by Holland and Gottfried (1955) and Murakami *et al* (1991).

The conventional pellet technique (Zhang *et al* 1996) was employed for powder absorption measurements. A small amount (3 mg) of powdered zircon was thoroughly mixed with 900 mg of dry CsI powder. 300 mg of the sample/matrix mixtures were pressed into disc-shaped pellets of 13 mm diameter at room temperature under vacuum. The same sample pellet was measured for both FIR and MIR regions within 12 hours of creation. For reflection measurements, gem quality zircon crystals were selected. The crystallographic orientations of the crystals were determined from the external morphology, X-ray precession techniques, and optical polarizing microscope. Crystal zircon plates were cut parallel to the $\boldsymbol{c}$-axis. The sample plates were then polished.

A Bruker IFS 113v spectrometer and a Bruker IFS 66v spectrometer were used to record IR spectra between 70 and 5000 cm^{-1}. A DTGS (for powder absorption measurement) and a liquid-nitrogen-cooled MCT (for reflectance measurement) detectors, coupled with a KBr beamsplitter and a Globar source were used to record the spectra between 450 and 5000 cm^{-1}. For the frequency region 70–700 cm^{-1}, a DTGS detector with a polyethylene window was coupled with a mercury lamp and a 3.5 μm or 6 μm Mylar beamsplitter. Using a commercial reflection accessory from Bruker we were able to perform close normal incidence measurements. A spectral resolution of 2 cm^{-1} was used for absorption measurements and 4 cm^{-1} for reflectance measurements. Gold mirrors were used as references for reflection spectra, and a KRS5 and a polyethylene wire-grid polarizors were employed. Kramers–Kronig analysis of the reflection spectra was performed to obtain dielectric constant as a function of frequency ω. The possible experimental errors that may affect IR analysis of powder absorption spectra have been discussed in detail by Zhang *et al* (1997). It was checked that the sum rule was obeyed so that the accuracy of the measured reflectivity was deemed sufficient for this study.

3. Analysis and results

3.1. IR absorption and polarized reflection spectra

For well crystallized zircon samples, all seven predicted infrared modes (internal $= 2A_u + 2E_u$ and external $= A_{2u} + 2E_u$) (Dawson *et al* 1971) were observed and their band frequencies and damping (the data obtained from reflection spectra) are listed in table 1. As predicted by the selection rules resonances of E_u symmetry are observed when the electric vector of the incident infrared radiation, $\boldsymbol{E}$, is perpendicular to the $\boldsymbol{c}$ axis while those of A_{2u} symmetry are observed when $\boldsymbol{E}$ is parallel to $\boldsymbol{c}$. Our data agree well with previous results from crystalline zircon (Dawson *et al* 1971, Gervais *et al* 1973). The IR spectrum of the SiO_4 group in zircon is characterized by Si–O stretching ν_3 (E_u mode at 885 cm^{-1} and A_{2u} mode at 989 cm^{-1}; and the phonon frequencies used here are obtained from the reflection spectrum), and O–Si–O bending ν_4 (E_u mode at 430 cm^{-1} and A_{2u} mode at 608 cm^{-1}). The three IR modes below 400 cm^{-1} are external modes. They are related to SiO_4 group motions against Zr atoms and motions of Zr atoms (Farmer 1975).

Radiation damage leads to systematic variations in the absorption spectrum of zircon: a decrease in band intensity, changes in peak frequency, line broadening and loss of spectral detail as well as a significant increase in additional absorption signals near 520, 680 and 1100 cm^{-1} (figure 1(a)). These additional signals, especially the features near 520 cm^{-1}, can be detected

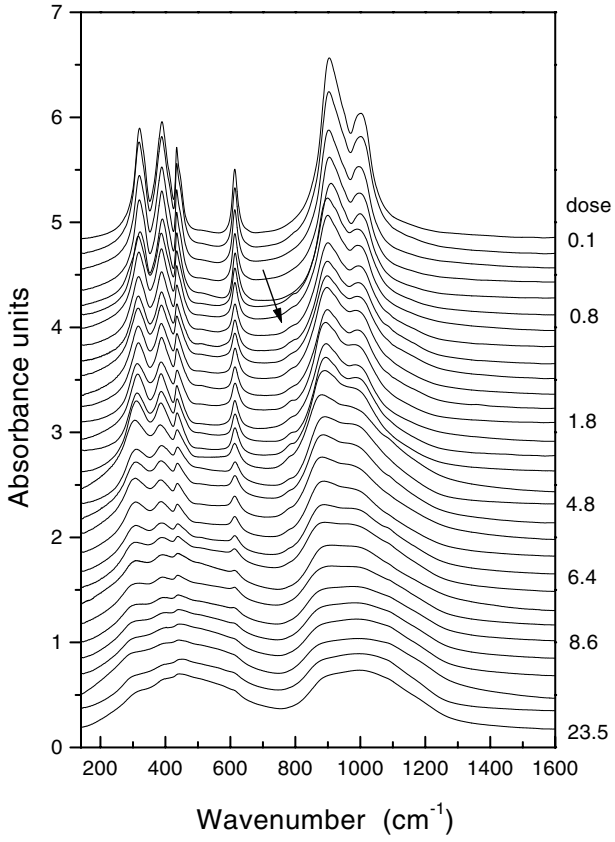

(a)

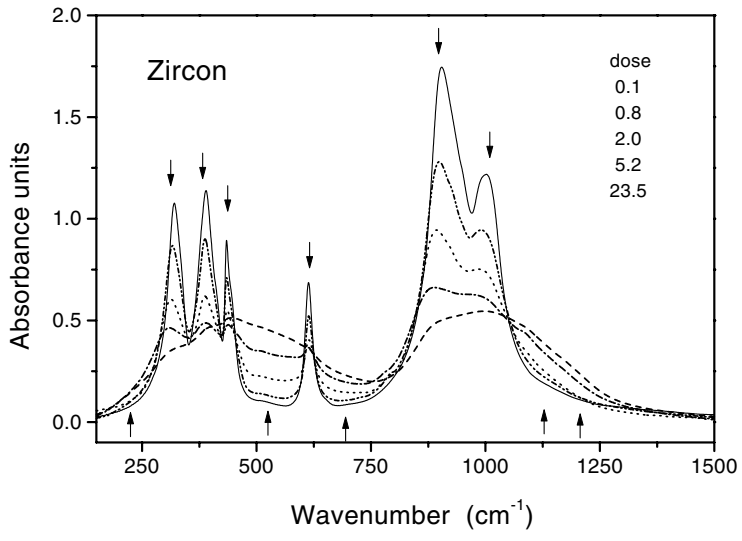

(b)

Figure 1. Effects of metamictization on the infrared spectrum of zircon. Stack plots of absorption spectra between 150 and 1600 cm^{-1} (a); absorption intensity variations (b). The arrows show the changes of absorbance due to metamictization. Radiation dosage is in units of 10^{18} α-events g^{-1}. An extra peak appears near 796 cm^{-1} in moderately damaged samples.

Table 1. Observed TO and LO modes of crystalline zircon sample (with dose of 1.0×10^{18} α-events g^{-1}). Frequency ω and damping Γ are in cm^{-1}. The band assignment is from Farmer (1975).

E_u ($\boldsymbol{E} \perp \boldsymbol{c}$)					A_{2u} ($\boldsymbol{E} \parallel \boldsymbol{c}$)				
ω_{TO}	Γ_{TO}	ω_{LO}	Γ_{LO}	Assignment	ω_{TO}	Γ_{TO}	ω_{LO}	Γ_{LO}	Assignment
282	7	351	7	rotatory	338	10	475	12	*trans*
385	9	416	7	*trans*	606	9	644	17	ν_4
431	5	470	3	ν_4	980	13	1101	15	ν_3
880	11	1030	12	ν_3					

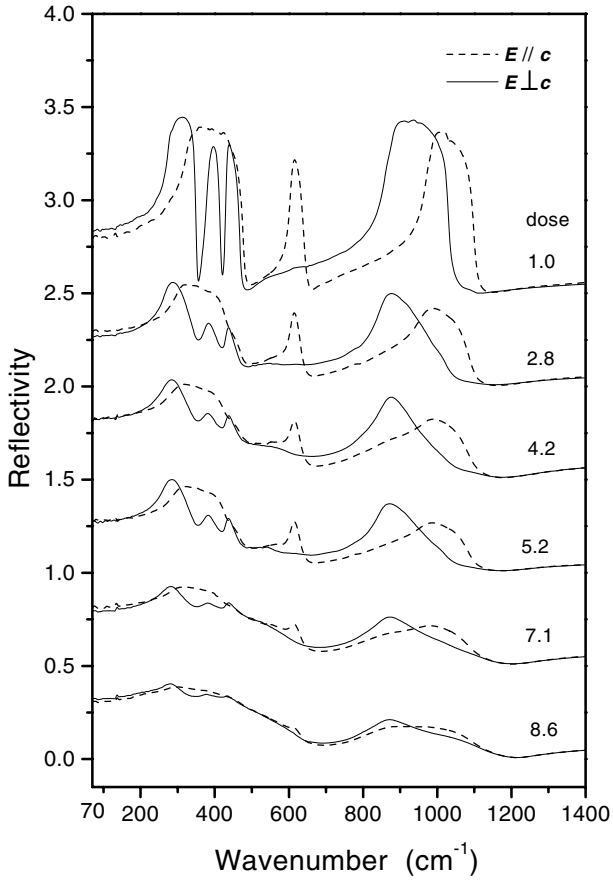

Figure 2. Stack plots of polarized reflection spectra of zircon between 70 and 1400 cm^{-1}. Radiation dosage is in units of 10^{18} α-events g^{-1}. The solid lines represent the spectra with $\boldsymbol{E} \perp \boldsymbol{c}$ (A_{2u} symmetry) and the dashed lines correspond to those with $\boldsymbol{E} \parallel \boldsymbol{c}$ (E_u symmetry). The extra 796 cm^{-1} peak appears in the sample with a dose of 2.8×10^{18} α-events g^{-1}.

in samples with dose as low as 1.5×10^{18} α-events g^{-1}. These extra features existed in all heavily damaged samples and their intensity showed a continuous increase with increasing dose. This continuous intensity increase is an indication of the appearance of the amorphized phase (figure 1(b)). It is very surprising that some characteristic spectral features of crystalline zircon still persist in highly damaged samples. Especially, the most damaged sample (with dose of 23.5×10^{18} α-events g^{-1}) studied, still gives local absorption maxima near 305, 385, 450, 607 cm^{-1} where IR peaks appear in well crystallized zircon (figure 1(a)).

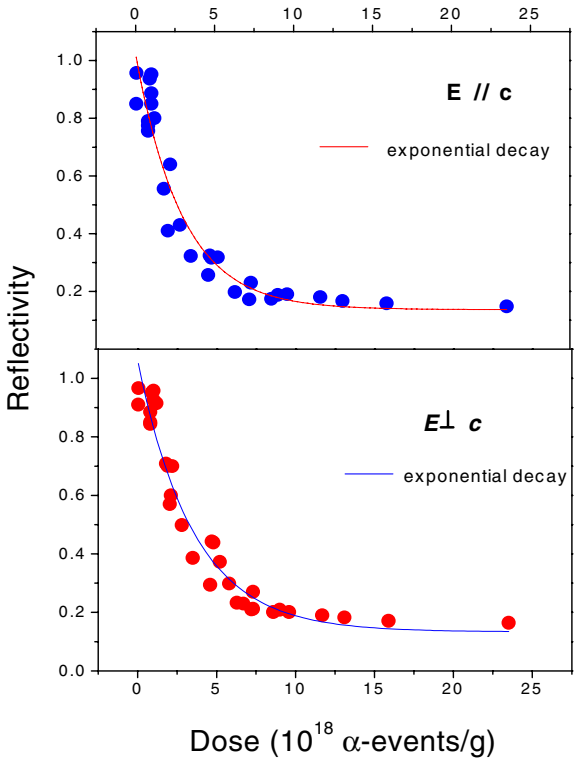

Figure 3. Reflectivity at 995 cm^{-1} ($\boldsymbol{E} \parallel \boldsymbol{c}$) and the height of the maximum near 850 cm^{-1} ($\boldsymbol{E} \perp \boldsymbol{c}$) as a function of radiation dose. The data were obtained from Sri Lanka zircon samples. The data at dose higher than 10^{18} α-events g^{-1} were from unpolarized spectra as it is impossible to orientate those high-dose samples due to the radiation-damage-induced loss of anisotropy (see more details in text). The dose dependence of reflectivity can be used to determine radiation dose.

Polarized reflection spectra of zircons with different degrees of damage are shown in figure 2. The effects of metamictization in zircon are evidenced as a dramatic decrease in reflectivity and a loss of spectral details accompanied with an increase in reflectivity in the spectra with $\boldsymbol{E} \perp \boldsymbol{c}$ in the regions 480–600 cm^{-1} and 1050–1200 cm^{-1}. The dose dependence of the measured reflectivity at 995 cm^{-1} ($\boldsymbol{E} \parallel \boldsymbol{c}$) and near the maximum near 850 cm^{-1} ($\boldsymbol{E} \perp \boldsymbol{c}$) (figure 3) was obtained for Sri Lanka samples which were studied previously (Murakamii *et al* 1991, Ellsworth *et al* 1994, Salje *et al* 1999, Ríos *et al* 2000, Zhang *et al* 2000a, b, c). For the case of dose higher than 10×10^{18} α-events g^{-1}, the samples could not be oriented, because no Bragg reflections were found and these high-dose samples all had irregular external shapes. A crystal of the most damaged sample (dose $= 23.5 \times 10^{18}$ α-events g^{-1}) was cut into a cube and polarized reflection measurements were performed on its three perpendicular surfaces. The polarized spectra obtained from these different planes with different polarization conditions showed essentially identical spectral features (Zhang *et al* 2000b) within the experimental resolution. Therefore, for these high-dose samples the data in figure 3 obtained from unpolarized spectra are reliable. The implication of the correlation between reflectivity and the spectral features of IR signals and degree of radiation dose in zircon is that it may be used for the determination of the degree of damage from IR spectra.

One of the important spectral variations is the appearance of an absorption peak near

796 cm^{-1} in moderately damaged zircon samples (as indicated by an arrow in figure 1(a)). In contrast to the new features in the regions near 520, 680 and 1100 cm^{-1} that showed an increase of intensity with increasing dose, this signal did not appear in well crystallized samples (e.g. samples with doses less than 0.8×10^{18} α-events g^{-1}), but it was detected in all samples with intermediate degrees of damage. For samples with doses between 1.5 and 6.5×10^{18} α-events g^{-1}, this peak appeared to have similar values of intensity. With further increasing dose, this peak becomes weaker, and eventually undetectable in the heavily damaged samples (e.g. samples with dose of 9.6 and 23.5×10^{18} α-events g^{-1}) (figure 1(a)). This peak also showed as a weak local maximum in the reflection spectra of a sample (dose $= 2.8 \times 10^{18}$ α-events g^{-1}) with $\boldsymbol{E} \parallel \boldsymbol{c}$ and $\boldsymbol{E} \perp \boldsymbol{c}$ (figure 2). The peak could hardly be seen in reflection spectra of other samples, probably due to the relatively low sensitivity and resolution of the reflectance measurements. This peak has appeared in some IR spectra reported previously (e.g. Vance 1975, Woodhead *et al* 1991) although it did not seem to have drawn some authors' attention. It was also observed in the reflection spectra of moderately damaged zircon annealed at high temperatures (Zhang *et al* 2000b). According to theoretical and experimental work (Dawson *et al* 1971), the $ZrSiO_4$ structure does not have an IR band near 796 cm^{-1}. Why moderately damaged samples all show this relatively sharp peak is unclear. It has been proposed that it could be due to a radiation-induced intermediate phase or the structural distortions near the boundaries between the amorphized and crystalline regions (Zhang *et al* 2000b, c).

3.2. Dielectric constants, TO and LO phonon response

The dielectric function ($\varepsilon(\omega) = \varepsilon'(\omega) + i\varepsilon''(\omega)$) and dielectric loss ($-\mathrm{Im}(1/\varepsilon) = \varepsilon''/(\varepsilon'^2+\varepsilon''^2)$) (figures 4(a)–4(c)) were obtained through Kramers–Kronig analysis of the measured reflection spectra. The accuracy of the experimental data was checked using the sum rule (Brüesch 1986):

$$\int_0^{\omega_0} \frac{\varepsilon''(\omega)}{\omega}\,\mathrm{d}\omega = \frac{\pi}{2}(\varepsilon_0 - \varepsilon_\infty) \tag{1}$$

where ε_0 and ε_∞ are the static and high-frequency dielectric constants, respectively while ω_0 is a frequency which high enough to include all vibrational modes in the integral. The integration was performed between 70 and 5000 cm^{-1} for crystalline zircon. The left hand side of expression (1) gives values of 13.3 ($\boldsymbol{E} \perp \boldsymbol{c}$) and 13.7 ($\boldsymbol{E} \parallel \boldsymbol{c}$) in good agreement with $\pi(\varepsilon_0 - \varepsilon_\infty)/2 = 11.6$ with use of $\varepsilon_0 = 11.2$ and $\varepsilon_\infty = 3.8$ (Gervais *et al* 1973). This indicates that the reflectance measurements and Kramers–Kronig analysis yield reliable absolute data. For a crystalline sample (e.g. dose $= 1.0 \times 10^{18}$ α-events g^{-1}) the values of dielectric constants and dielectric loss agree very well with reported data (Dawson *et al* 1971, Gervais *et al* 1973). The effects of radiation damage on the dielectric function are characterized by a continuous decrease in their value and a loss of details with increasing dose. However, a systematic increase in ε'' appears between 500 and 800 cm^{-1}, and this corresponds to the formation of the amorphous phase indicated by absorption spectra. Interestingly, the static dielectric constant ε_0 remains almost unchanged with a value of 11 ± 1 for all radiation doses studied in contrast to dramatic and continuous changes of ε' and ε'' in higher frequency ranges.

The frequency of TO (transverse optical) phonons are given by peak positions in ε'' while LO (longitudinal optical) phonon frequencies can be obtained from the maxima of the dielectric loss function, $-\mathrm{Im}(1/\varepsilon) = \varepsilon''/(\varepsilon'^2+\varepsilon''^2)$. It has been established that for a multimode crystal LO and TO modes with small damping follow the Lyddane–Sachs–Teller (LST) relation (Lyddane *et al* 1941):

$$\frac{\varepsilon_0}{\varepsilon_\infty} = \prod_i \frac{\omega_i^2(\mathrm{LO})}{\omega_i^2(\mathrm{TO})} \tag{2}$$

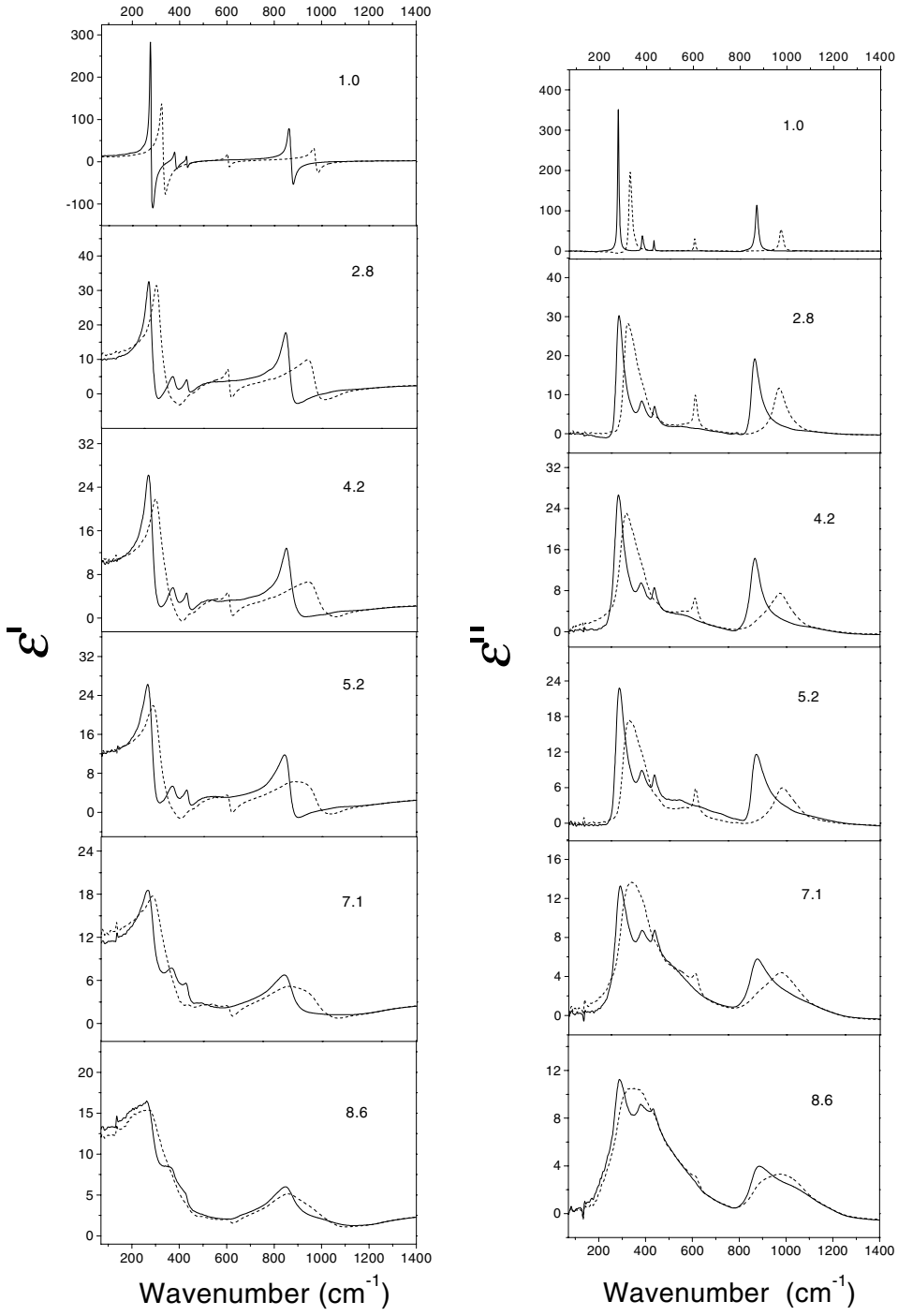

Figure 4. The wavenumber dependence of dielectric function and energy loss function of damaged zircon samples: ε', the real part of the dielectric constant (a); ε'', the imaginary part of the dielectric constant (b), and $-\mathrm{Im}(1/\varepsilon)$, the energy loss function (c). The solid lines show the data with $\boldsymbol{E} \perp \boldsymbol{c}$ and dashed lines correspond to those with $\boldsymbol{E} \parallel \boldsymbol{c}$. The radiation dosage indicated is in units of 10^{18} α-events g^{-1}.

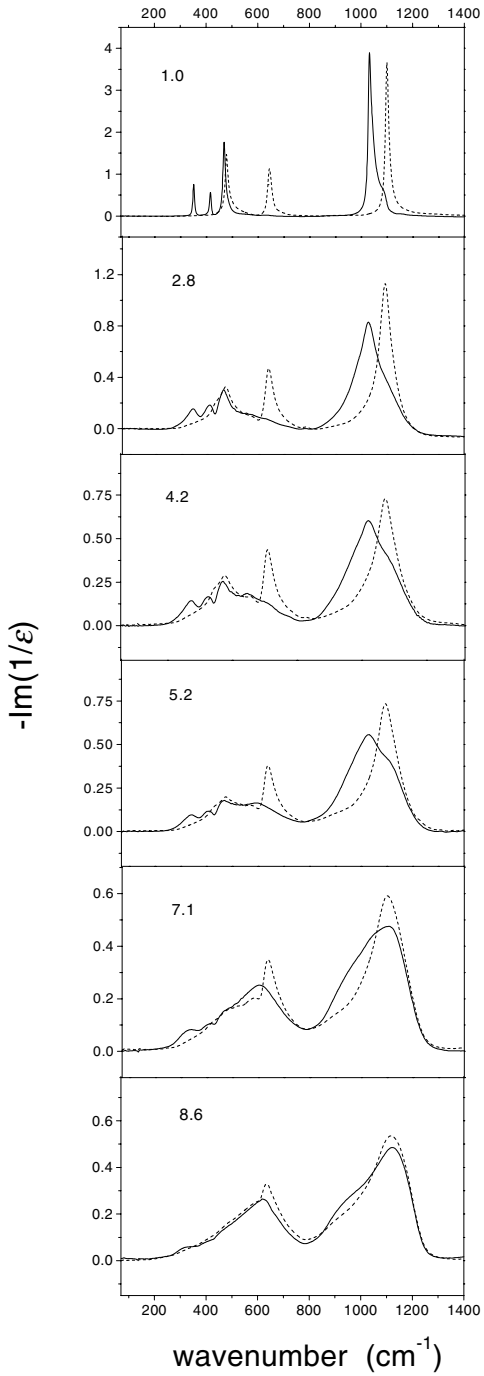

(c)

Figure 4. (Continued)

Using the data in table 1, the right hand side of expression (2) gives values of 2.9 for $\boldsymbol{E} \perp \boldsymbol{c}$ 2.8 for $\boldsymbol{E} \parallel \boldsymbol{c}$ which are in very good agreement with $(\varepsilon_0/\varepsilon_\infty) = 2.9$.

3.3. Effective medium approach

Experimental observations have suggested that damaged zircon contains a random network of crystalline and amorphized phases (Murakamii *et al* 1991, Salje *et al* 1999, Capitani *et al* 2000). One can treat the radiation-damaged zircon as a mixture of amorphous and damaged crystalline zircons with a first approximation—ignoring the interaction between amorphous areas and damaged crystalline areas. We analysed the measured spectra using the effective medium approach (Maxwell-Garnett 1904, Granqvist and Hunderi 1978, Yagil *et al* 1995) as follows:

$$\varepsilon_e = \varepsilon_{amorphous}\left(1 + (2/3)\sum_i f_i\alpha_i\right)\left(1 - (1/3)\sum_i f_i\alpha_i\right)^{-1} \tag{3}$$

with

$$\alpha_i = \frac{\varepsilon_{crystalline} - \varepsilon_{amorphous}}{L_i\varepsilon_{crystalline} + (1 - L_i)\varepsilon_{amorphous}} \tag{4}$$

where ε_e is the effective dielectric response of the measured damaged zircon samples, $\varepsilon_{amorphous}$ and $\varepsilon_{crystalline}$ are dielectric responses of the amorphized and crystalline phases and f_i and L_i are, respectively, the volume fraction and the depolarization factor of a subset of the crystalline domains with similar geometry. For spheres $L = 1/3$, $L < 1/3$ for a platelike spheroid and $L > 1/3$ for needle-like ones. In the present calculation, the value $L = 1/3$ was used. The above expressions are suitable for the case of heavily damaged samples (i.e. the fraction of the amorphized phase is the dominate component). For the case of weakly damaged samples, the above expressions should be modified accordingly.

The choice of $\varepsilon_{crystalline}$ and $\varepsilon_{amorphous}$ is an important aspect in applying the effective medium approach in radiation-damaged zircon. The spectrum of undamaged zircon is not suitable for $\varepsilon_{crystalline}$ in moderately and heavily damaged samples and $\varepsilon_{crystalline}$ appears to change with radiation dose. For instance, Raman measurements have shown that frequencies of Raman bands from crystalline parts in damaged zircon decrease dramatically in the region 0–2.5 $\times$ 10^{18} α-events g^{-1} and they become saturated at higher doses (Zhang *et al* 2000c). In addition, experimental data have also shown that the cell parameters a and c, which are related to crystalline parts in damaged zircon, increase with increasing radiation dose and they saturate at doses higher than 3.0–3.5 $\times$ 10^{18} α-events g^{-1} (Holland and Gottfried 1955, Murakamii *et al* 1991, Weber *et al* 1994, Salje *et al* 1999). The work of Murakamii *et al* (1991) has also shown that the undamaged zircon phase does not exist in moderately and highly damaged samples. Therefore, for samples with different degrees of damage, different $\varepsilon_{crystalline}$ are needed for the analysis of the measured spectra. In order to make further checks, spectral substitution was performed to remove the individual spectra of the two extremes (i.e. the most undamaged and the most damaged zircon) from the measured spectra. We noted that removing the spectrum of the most undamaged sample did not produce a meaningful difference spectrum (i.e. negative absorbance, strange spectral shapes and unusual baselines) when radiation dose was higher than 1.5 $\times$ 10^{18} α-events g^{-1}. This suggests that there is no significant amount of undamaged zircon in those samples. However, subtracting the spectrum of the most damaged sample appeared to produce reasonable difference spectra, as shown in figure 5. Although the structure of the amorphized phase might change from low to high dose, the difference spectra (figure 5) appear to suggest that any potential changes in the IR spectra are probably not significant. We obtained $\varepsilon_{crystalline}$, the dielectric response of crystalline parts, as a first approximation, through curve-fitting the measured spectra to Lorentzian functions. The fitting was performed in three frequency ranges: 240–480 cm^{-1}, 575–660 cm^{-1} and 835–1060 cm^{-1} with individual linear baselines. These ranges were chosen to assure only the up-parts of the

sharp peaks were fitted in order to extract the principal contributions of the crystalline phase and to exclude the broad signals from the amorphized phase. The peak parameters obtained through the fitting were used to produce the secondary spectra (Zhang *et al* 1997) mainly reflecting the crystalline phase at different dosage. In order to gain correct intensities the secondary spectra were then normalized against that of the most damaged sample, using the integrated absorbance in the region between 150 and 1500 cm^{-1}, as the values of ε_0 did not show a significant change between crystalline and heavily damaged zircons. For the case of dose higher than 3.0×10^{18} α-events g^{-1}, curve-fitting the sharp lines became difficult due to the dramatic decrease of the fraction of the crystalline phase in the samples. For this case, $\varepsilon_{crystalline}$ was obtained through removing the spectrum of the most damaged sample (with dose of 23.5×10^{18} α-events g^{-1}) from that of a moderately damaged sample with a dose value of 2.9×10^{18} α-events g^{-1}. The difference spectrum was then normalized against that of the most damaged sample. This sample was chosen because its dose is close to 3.0–3.5 $\times 10^{18}$ α-events g^{-1}, the value above which cell parameters and Si–O Raman bands become saturated. The spectrum of the most damaged sample (23.5×10^{18} α-events g^{-1}) in this study was used as $\varepsilon_{amorphous}$ in whole dose range, i.e. it was assumed that $\varepsilon_{amorphous}$ was dose independent. Simulations have shown that the damaged materials appear less able to resist further damage (Trachenko *et al* 2001) and the local configuration of the amorphized phase could undergo further modifications. The reasonable outcomes of the spectral subtraction as shown in figure 5 suggest that the related spectral changes could be very subtle or infrared data do not appear very sensitive to the changes of $\varepsilon_{amorphous}$ with increasing dose. Experimental results have shown that the amorphized phase of damaged zircon exhibits similar Raman spectra features for high-dose cases (dose $\gg 3.5 \times 10^{18}$ α-events g^{-1}) (Zhang *et al* 2000c). The possible changes of $\varepsilon_{amorphous}$ are expected to occur in the low-dose range where $\varepsilon_{amorphous}$ plays a less important role in the effective dielectric response ε_e and they might not significantly affect the effective medium analysis. Calculated results from effective medium approach show good agreements with those measured spectra of heavily damaged samples (figure 6). This implies that the choosing of $\varepsilon_{crystalline}$ and $\varepsilon_{amorphous}$ is reasonable.

3.4. Fraction of amorphized phase

The dose-dependence of f, the fraction of the amorphized phase, was extracted through comparing the results from the effective medium calculation and the measured data (figure 7) as well as by spectral subtraction. The absorption signals near 520, 680 and 1100 cm^{-1} (figure 1(a)) are considered as characteristic bands from the amorphous phase because they are absent in undamaged samples and show significant increase with increasing radiation dose. As described in the previous section, the spectrum of the most damaged sample was removed from the measured spectra and the subtraction was performed in such a way as to avoid over-subtraction and meaningless results (figure 5). The uncertainty of determination of the fraction of the amorphized phase through using the effective medium approximation could be mainly related to the choice of $\varepsilon_{amorphous}$ and $\varepsilon_{crystalline}$. As described in the previous section, the successful application of the effective medium approach to the measured spectra implies that they are good approximations. The results obtained from IR methods are consistent with recent results from X-ray diffraction (R´ios *et al* 2000) and NMR (Farnan and Salje 2001). The good agreements among IR, XRD and NMR data further suggest that $\varepsilon_{amorphous}$ and $\varepsilon_{crystalline}$ were reasonably well chosen. The dose dependences of the fraction obtained from IR support direct impact damage in zircon (Ríos *et al* 2000) and are consistent with the hypothesis that amorphization is produced in cascades.

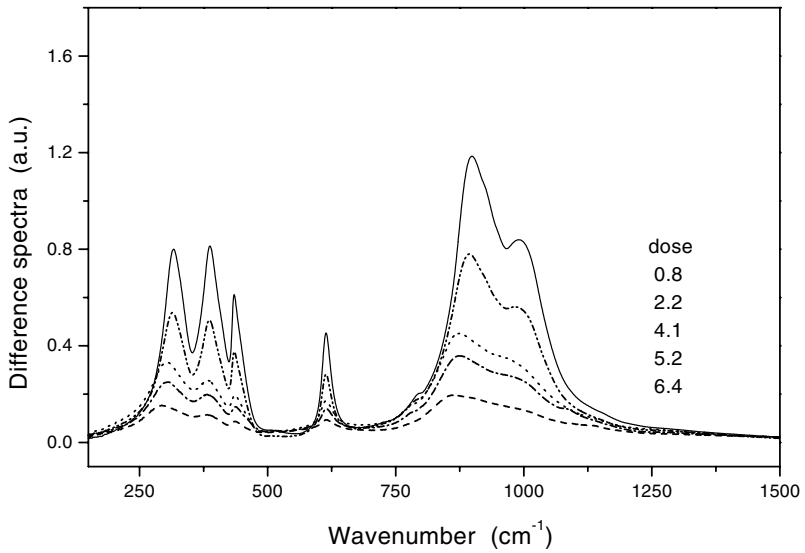

Figure 5. Difference spectra after removing the spectrum of the most damaged zircon (23.5×10^{18} α-events g^{-1}).

4. Discussion

The key issue regarding extracting information about the local structural configurations of the amporphized phase from the IR data is to understand why for zircon samples with a dose as high as 23.5×10^{18} α-events g^{-1} the IR band of crystalline zircon below 400 cm^{-1} still remains active, whereas additional absorption signals appear in the Si–O stretching region (800–1300 cm^{-1}) as well as the Si–O bending region (∼400–650 cm^{-1}). These IR bands below 400 cm^{-1} mainly correspond to Zr–O interactions at a first approximation (Woodhead *et al* 1991). The frequencies of the bands are generally determined by cation–oxygen forces (Farmer 1975) in the crystal structure of $ZrSiO_4$. The observation that the IR bands below 400 cm^{-1} still persist in highly metamict samples suggests that to some extent the local environments for Zr atoms may not be very different from those in crystalline $ZrSiO_4$, i.e. local order may exist in the amorphized phase. This observation supports a recent atomic modelling of radiation damage in zircon (Trachenko *et al* 2001). It is obvious that the IR data cannot be simply explained by a complete breaking down of ZrO_8 in the amorphized phase because this would lead to significant changes of band frequencies and the number of bands below 400 cm^{-1}.

The appearance of the extra absorption signals in the regions of 400–650 cm^{-1} and 900–1200 cm^{-1} in heavily damaged samples, however, suggests that metamictization in zircon does cause changes to the local structure from that of crystalline $ZrSiO_4$. We interpret these radiation-induced additional IR signals as a formation of new Si–O-Si linkages or an appearance of high-Q species in the amorphized phase for the following reasons. Previous investigations have shown some correlations between observed Si–O vibrational bands and their local structure environments (McMillan 1984), although how to assign IR and Raman bands in glasses and disordered materials that lose translational and orientational correlations is under debate. In silicates, a polymerization of silicon oxygen tetrahedra normally leads to two significant effects on the spectra. Firstly, the degeneracy of some Si–O stretching vibrations may be lifted, causing the spectrum to become more complex. As a result of the differences

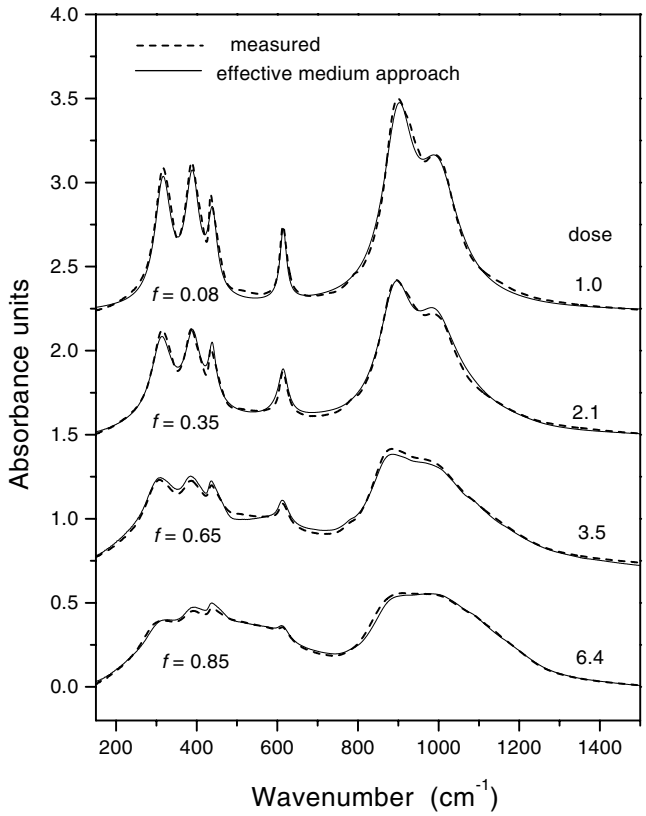

Figure 6. Comparison of the spectra calculated from the effective-medium approach and those measured.

between the bonding of the non-bridging oxygen and the bridging oxygen, additional Si–O stretching bands may appear in the region 950–1200 cm^{-1}. Secondly, new types of Si–O bending band may appear in the region between 500 and 750 cm^{-1} as the result of the occurrence of new Si–O–Si angles. Their exact positions depend on the corresponding Si–O–Si angles. Therefore, several Si–O bending bands may occur in the spectrum of a mineral in which there are several Si–O-Si angles. All this may involve breaking bonds, displacements of atoms and reorientation of original silica oxygen tetrahedra caused by α-decay damage, producing new structural units and chains. This observation is consistent with a recent simulation of radiation damage in zircon (Trachenko *et al* 2001). Therefore, the local configuration of the metamict state probably contains newly formed Si–O-Si linkages plus local order of the original structure to some degree.

5. Conclusion

IR spectroscopy has been used to investigate the metamictization process and the metamict state in zircon. Extra IR signals in the regions of 400–650 cm^{-1} and 900–1200 cm^{-1} were observed and their appearances suggest new Si–O-Si linkages or Si–O–Si angles related to high-Q species and polymerization. IR bands of crystalline zircon in the far-infrared region still persist in highly metamict samples. This implies that some local order or short-range order persists around Zr in the amorphized phase. The dielectric function ($\varepsilon = \varepsilon' + i\varepsilon''$) and

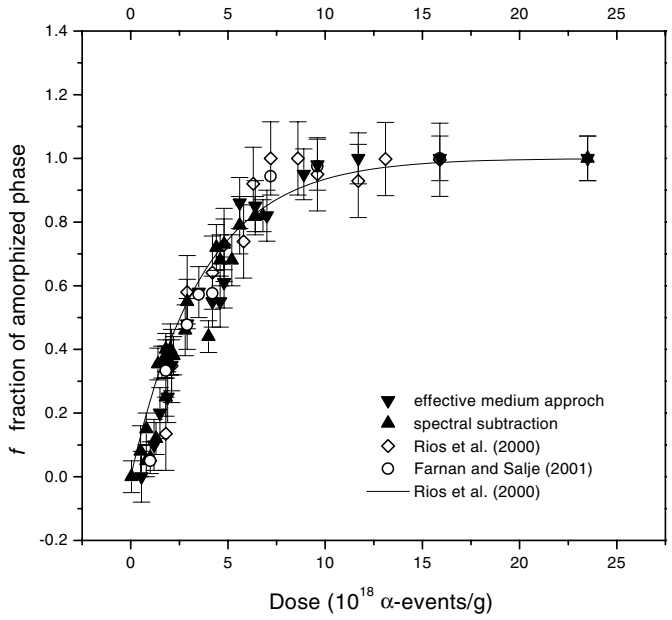

Figure 7. Dose dependence of the fraction of the amorphized phase. The down-triangle symbols indicate the data obtained from the effective medium approach and the up-triangles from the spectral subtraction method described in the text. The open symbols represent data from XRD (Ríos *et al* 2000) and NMR (Farnan and Salje 2001). The line is the function $f = 1 - \mathrm{e}^{-B_a D}$ where D is radiation dose and $B_a = 2.7(3) \times 10^{-19}$ g is the amount of amorphous material produced per alpha-recoil (Ríos *et al* 2000).

energy loss function ($-\mathrm{Im}(1/\varepsilon)$) were obtained through Kramers–Kronig analysis. Radiation damage causes continuous variations of the dielectric constant and energy loss function. The effective-medium approach was used to calculate the IR spectra of heavily damaged samples and the results show a good agreement with the measured data. The results show that IR signals of damaged zircons consist of at least two principal components: one with broad spectral features from the amorphized/metamict material and the other with sharper lines from distorted crystalline or damaged crystalline regions. The former increases in its intensity with increasing dose while the latter decreases in intensity. The signals from the amorphized phase have been detected in samples with radiation dose as low as 1.5×10^{18} α-events g^{-1}. The dose dependence of the fraction of the amorphized phase was extracted through the effective-medium approach and spectral subtraction and the results show good agreements with those obtained by XRD and NMR.

Acknowledgments

The authors would like to thank Andrew Clark, Mark Welch at the Natural History Museum (London, UK), Rodney C Ewing at Department of Nuclear Engineering and Radiological Sciences and Department of Geological Sciences (University of Michigan, USA), Steve Laurie at the Sedgwick Museum (University of Cambridge, UK), and Jochen Schlüter at the Mineralogisches Museum (Universität Hamburg, Germany) for providing some of the samples used in this study. Thanks are due to William Lee for reading the original manuscript.

References

Brüesh P 1986 *Phonons: Theory and Experiments. II Experiments and Interpretation of Experimental Results* (Berlin: Springer) p 29

Capitani G C, Leroux H, Doukhan J C, Ríos S, Zhang M and Salje E K H 2000 *Phys. Chem. Mineral.* **27** 545

Dawson P, Hargreave M M and Wilkinson G F 1971 *J. Phys. C: Solid State Phys.* **4** 240

Ellsworth S, Navrotsky A and Ewing R C 1994 *Phys. Chem. Mineral.* **21** 140

Ewing R C 1994 *Nucl. Instrum. Methods Phys. Res.* B **91** 22

Farges F and Calas G 1991 *Am. Mineral.* **76** 60

Farmer V C 1975 Orthosilicates, prosilicates, and other finite-china silicates *The Infrared Spectra of Minerals* ed V C Farmer (London: Mineralogical Society) p 286

Farnan I and Salje E K H 2001 *J. Appl. Phys.* **89** 2084

Gervais F, Piriou B and Cabannes F J 1973 *J. Phys. Chem. Solids* **34** 1785

Granqvist C G and Hunderi O 1978 *Phys. Rev.* B **18** 2897

Hazen R M and Finger L W 1979 *Am. Mineral.* **64** 157

Holland H D and Gottfried D 1955 *Acta Crystallogr.* **8** 291

Lyddane R H, Sachs R C and Teller E 1941 *Phys. Rev.* **59** 673

Maxwell-Garnett C 1994 *Phil. Trans. R. Soc.* **203** 385

Mclaren A C, Fitz J D and Williams I S 1994 *Geochim. Cosmochim. Acta* **58** 993

McMillan P 1984 *Am. Mineral.* **69** 622

Murakamii T, Chakoumakos B C, Ewing R C, Lumpkin G R and Weber W J 1991 *Am. Mineral.* **76** 1510

Nasdala L, Irmer G, and Wolf D 1995 *Eur. J. Mineral.* **7** 471

Ríos S, Salje E K H, Zhang M and Ewing R C 2000 *J. Phys.: Condens. Matter* **12** 2401

Salje E K H, Chrosch J and Ewing R C 1999 *Am. Mineral.* **84** 1107

Trachenko K O, Dove M T and Salje E K H 2001 *J. Phys.: Condens. Matter* **13** 1947

Vance R E 1975 *Radiat. Effects* **24** 1

Weber W J, Ewing R C and Wang L M 1994 *J. Mater. Res.* **9** 688

Woodhead J A, Rossman G R and Silver L T 1991 *Am. Mineral.* **76** 74

Yagil Y, Baudenbacher F, Zhang M, Birch J R, Kinder H and Salje E K H 1995 *Phys. Rev.* B **52** 15 582

Zhang M, Salje E K H, Capitani G C, Leroux H, Clark A M and Schlüter J 2000a *J. Phys.: Condens. Matter* **12** 3131

Zhang M, Salje E K H, Carpenter M A, Parsons I, Kroll H, Reed S J B and Graeme-Barber A 1997 *Am. Mineral.* **82** 849

Zhang M, Salje E K H, Ewing R C, Farnan I, Ríos S, Schlüter J and Leggo P 2000b *J. Phys.: Condens. Matter* **12** 5189

Zhang M, Salje E K H, Farnan I, Graem-Barber A, Danial P, Ewing R C, Clark A M and Leroux H 2000c *J. Phys.: Condens. Matter* **12** 1915

Zhang M, Wruck B, Graeme-Barber A, Salje E K H and Carpenter M A 1996 *Am. Mineral.* **81** 92